Enantioselective Au(i)-catalyzed tandem reactions between 2-alkynyl enones and naphthols by the tethered counterion-directed catalysis strategy

Yunliang Yu, Nazarii Sabat, Meriem Daghmoum, Zhenhao Zhang, Pascal Retailleau, Gilles Frison, Angela Marinetti, Xavier Guinchard

The Enantioselective TCDC approach in Au(I)-Catalysis: Insights into the Reactions between 2-Alkynyl Ketones and Naphthols

Yunliang Yu, [a,b] Nazarii Sabat,[a,‡] Meriem Daghmoum,[a,‡] Zhenhao Zhang,[a,c] Pascal Retail-leau,[a] Gilles Frison,[c,d,*]Angela Marinetti,[a,*] and Xavier Guinchard[a,*]

[a] Université Paris-Saclay, CNRS, Institut de Chimie des Substances Naturelles, UPR2301, 91198 Gif-sur-Yvette, France.

[b] Université Paris-Saclay, CNRS, Institut de chimie moléculaire et des matériaux d'Orsay, 91405, Orsay, France.

[c] LCM, CNRS, Ecole Polytechnique, Institut Polytechnique de Paris, 91128 Palaiseau, France.

[d] Sorbonne Université, CNRS, Laboratoire de Chimie Théorique, 75005 Paris, France.

[‡] Equal contribution to this work.

* gilles.frison@polytechnique.edu; angela.marinetti@cnrs.fr ; xavier.guinchard@cnrs.fr

The enantioselective tandem cycloisomerization / addition reactions of 2-alkynyl enones with 1- and 2-naphthols have been investigated using gold(I) catalysts featuring hybrid phosphine-phosphoric acid ligands, according to the Tethered Counterion-Directed Catalysis strategy. The reactions occur at low catalytic loading (0.2-1 mol%), without silver additives, and the naphthols act as both *O*- and *C*-nucleophiles, leading to the corresponding addition products in high yields and enantioselectivities. Monitoring of the reaction course highlights both conversion of *O*-addition into *C*-addition products and racemization processes that can affect the enantiomeric excess of the final products. Examples of solvent-dependent enantiodivergence, as well as further conversion of the *C*-addition products into highly enantioenriched heteropolycycles are shown.

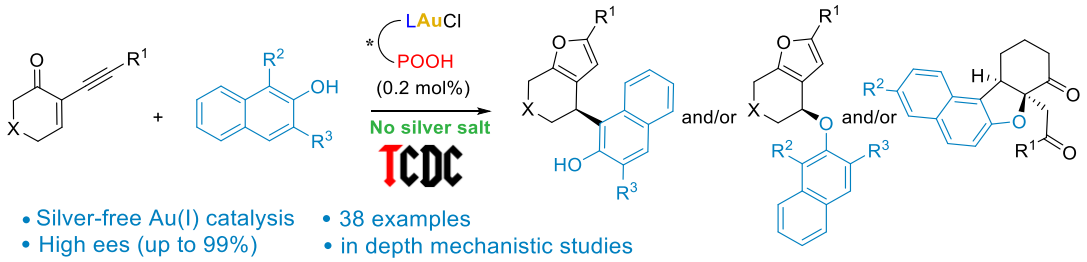

The field of Au(I) catalysis bloomed in the early 21st century and has now turned into an essential asset of transition metal catalysis for synthetic applications.[1] In particular, Au(I) complexes embedding either conventional or specifically designed chiral ligands have revealed high potential for enantioselective catalysis.[2, 3] As an alternative to these ligand-based approaches, Toste pioneered the use of Au(I) complexes bearing phosphates as chiral counterions,[4] according to the principle of Asymmetric Counterion-Directed Catalysis.[5] This strategy has encountered remarkable success, mainly in the intramolecular hydrofunctionalization of alkynes and allenes,[4, 6] likely because of the tight Au(I)/phosphate ion pairing, the steric bulk of the phosphate and the additional assistance of H-bonding between the substrates and the counterion in the key intermediates. Thus, with the aim to expand the scope of ACDC in gold catalysis, we have designed recently a new family of gold catalysts, the (CPAPhos)AuCl complexes, in which gold is tethered to its chiral phosphate counterion.[7] We have demonstrated that the tether can increase the geometrical constraints and decreases the flexibility of the key intermediates, and finally improves the stereocontrol in the catalytic reactions. These catalysts have been applied successfully to the dearomatization of naphthols with allenamides,[7b] as well as to the tandem cycloisomerization of 2-alkynyl enones / nucleophilic addition reactions.[7a, 7c, 8,9] In these last reactions (Scheme 1, eq. 1) that involve carbocation-phosphate pairs as key intermediates, the CPAPhos based catalysts led to high enantiomeric excesses at low catalysts loadings (0.2 mol%) using a variety of nucleophiles including indoles and nitrones.[7a, 7c] Among others, phenol had been used in these experiments where it behaved as an *O*-centered nucleophile.

Scheme 1: Context of this work: enantioselective tandem yne-enone cycloisomerization/nucleophilic additions under Ag(I) and Au(I)-catalysis

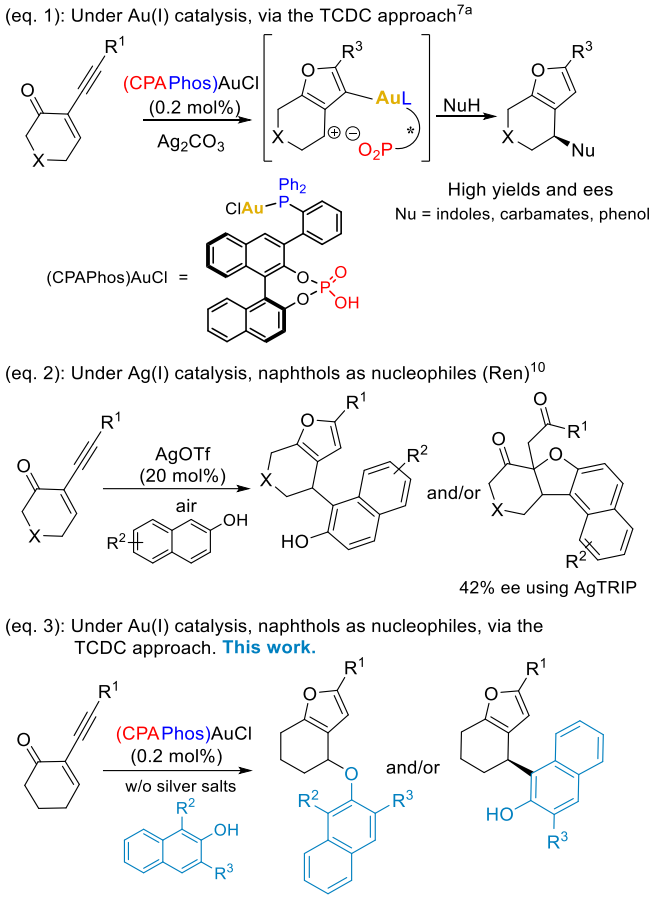

On the other hand, Xu and Ren have reported on analogous tandem reactions involving 2-naphthols as nucleophiles, taking place under silver trifluoroacetate catalysis.[10] These reactions afforded furanes **5** that result from the addition of naphthols as *C*-centered nucleophiles. The corresponding oxidation products **8** have been isolated as well (Scheme 1, eq. 2). A single attempt to run enantioselective variants using a chiral silver phosphate (AgTRIP), led to the final product **8** in only moderate, 42% ee. Thus, intrigued by the divergent behavior of phenol under gold catalysis, with respect to 2-naphthol under silver catalysis (*O*- vs *C*-additions, Scheme 1, eq. 1 and 2), we embarked in a systematic investigation on the use of 1- and 2-naphthols in the tandem reactions above, in order to enlighten these regioselectivity issues.

Moreover, based on our preliminary results, we were quite confident on that the (CPAPhos)AuCl based, TCDC approach might provide efficient enantioselective variants of these reactions (Scheme 1, eq. 3). Thus, the first aim of this work has been to investigate the applicability of the TCDC strategy to the enantioselective tandem cycloisomerization / naphthol addition reactions on cyclic α-ethynyl-enones. Within these studies, we have investigated in depth regio- and stereoselectivity issues of these apparently simple but actually quite complex reactions. The main results of these studies are summarized hereafter.

We have considered first the reactions of cyclic α-ethynyl-enones with 1,3-disubstituted 2-naphthols that are expected to behave as *O*-nucleophiles. The reaction conditions have been optimized using α-phenylethynyl-cyclohexenone **1a** and 1,3-dimethyl-2-naphthol **2a** as the substrates, in the presence of the (CPAPhos)AuCl catalysts (Table 1). The reactions were carried out initially in DCM, at rt, using 1 mol% of (CPA-Phos^{A})AuCl **3a**[7a] or (CPAPhos^{B})AuCl **3b**,[7c] in the presence of 0.5 mol% of silver carbonate. Catalyst **3a** delivered the bicyclic furan **4a** in 90% yield and 66% ee (entry 1), while catalyst **3b** that features a 3,5-$(CF_3)_2C_6H_3$ substituted binaphthyl moiety, led to a significantly improved 86% ee (entry 2).

With catalyst **3b,** the reaction could be carried out also in the absence of silver carbonate, with similar levels of catalytic activity and enantioselectivity (entries 3 vs 2), showing that previous activation of **3b** is not essential. After further optimization of the reaction temperature (0 °C), solvent (toluene) and concentration (0.1 M) the desired product **4a** was obtained in excellent yield (93%) and ee (95% ee), at the exceptionally low catalyst loading of 0.2 mol% (entry 8). The scope of the reaction was investigated then under the optimized conditions above, using (CPAPhos^{B})AuCl **3b** (0.2 mol%) as the catalyst, with both 2-naphthols and 1-naphthols as nucleophiles (Scheme 2).

Table 1: Optimization of the reaction between 1a and 1,3-dimethyl-2-naphthol

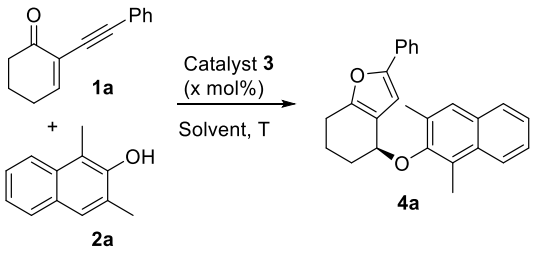

entry	catalyst	solvent	T °C	yield **4a** (%)[a]	ee **4a** (%)[b]
1[c]	**3a** (1)	DCM	rt	90	66
2[c]	**3b**(1)	DCM	rt	68	86
3	**3b** (1)	DCM	rt	65	87
4	**3b** (1)	DCM	0	99	90

5	**3b** (1)	DCM	-10	44	90
6	**3b** (0.2)	DCM	0	94	88
7	**3b** (0.2)	PhMe	0	92	91
8[d]	**3b** (0.2)	PhMe	0	93	95

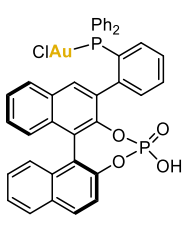

(*S*)-**3a**
(CPAPhos[A])AuCl

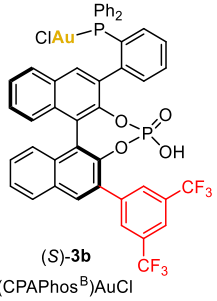

(*S*)-**3b**
(CPAPhos[B])AuCl

[a] Isolated yields. [b] Enantiomeric excesses were measured by chiral HPLC. [c] Reactions performed in the presence of Ag_2CO_3 (0.5 mol%). [d] Reaction performed at 0.1 M.

Starting from 2-naphthols with different combinations of methyl, ethyl and benzyl groups as R^2/R^3 substituents, the reaction afforded **4b-e** in excellent enantioselectivities (>93% ee). Monosubstituted naphthols (R^3=H) with methyl, ethyl and acetyl R^2 groups generated **4f-h** in high yields and enantioselectivities (86-93% ee). However, a benzyl group led to a drop of the enantiomeric excess (**4i**, 22% ee).

Next, the reactions between the α-yne-enone **1a** and various 2-substituted 1-naphthols were implemented. The 2-Me, allyl and *n*-Pr substituted naphthols **2**, resulted in the formation of **4j-l** in high yields (66-92%) and enantioselectivities (80-87% ee). This showed that 1-naphthols may be suitable substrates also, although they give slightly lower ees than 2-naphthols.

In a second series of experiments, the yne-enone substrates **1** were varied. The R^1 group was changed from phenyl to both substituted aryls and alkyl groups. The reactions of **2a** with *p*-chlorophenyl- and *p*-tolyl-substituted yne-enones **1b** and **1c** proceeded smoothly and delivered **4m** and **4n** with 96% ee, in the presence of silver carbonate. The introduction of an ester group on the phenyl substituent deactivates totally the substrate and therefore the starting material remains intact, either in the presence or absence of silver carbonate. For R^1 = alkyl, the reaction with the 2-naphthol **2a** led to compounds **4p-r** in good yields, but moderate enantioselectivity (39-55% ee). Similarly, moderate ees were obtained from the reactions of alkyl-substituted enones with 2-allyl-1-naphthol (**4t**, 28% ee and **4u**, 54% ee).

Finally, the 6-membered ring of the yne-enone **1a** could be replaced by a 7-membered ring, giving the bicyclic furane **4s** in 91% yield and 81% ee.

Following the successful use of substituted naphthols, we have considered the parent 2-naphthol and 1-naphthol as possible nucleophiles. These reactions might be more challenging, considering that these naphthols might react not only as *O*- but also as *C*-nucleophiles,[11] as illustrated by a wide range of electrophilic naphthol dearomatization processes.[12] Indeed, the reaction of enone **1a** with 2-naphthol **2m**, under various conditions, afforded initially mixtures of the *O*-addition product **6am**, the *C*-addition product **5am** and possibly the *C,O*-double addition product **7a**. A representative set of experiments is displayed in Table 2, other data are reported in the SI. Most of the experiments were carried out with a **1a**:**2m** 1:1 ratio, since an excess of ketone **1a** leads to the preferential formation of the *C,O*-double addition product **7a** (see SI).

A number of parameters proved to modulate both the **5am:6am:7a** ratios and the enantioselectivity levels, in a quite complex and interdependent way. Especially, the reaction outcomes proved to be strikingly time dependent. For instance, the reaction performed with catalyst **3a** in CH_2Cl_2 over 2 min (entry 1) afforded a 63:37 ratio of the *O*- and *C*-addition products, with total conversion. The ees of both products were high, with 82% ee and 92% ee for **6am** and **5am** respectively. Under the same conditions but after 30 min, the **6am**:**5am** ratio decreased to 43:57 and the ees also decreased concurrently (60% ee for **6am** and 70% ee for **5am**, entry 2). The same trend was observed with catalyst **3b**, as shown in entries 3 and 4. This catalyst provided the best conditions for the synthesis of **5am**, in terms of conversion rate and ee, at an intermediate 5 min reaction time, by decreasing the temperature to 10 °C (entry 5). Since reactions in CH_2Cl_2 are extremely fast and the ees erode with time, the optimal workup protocol involves rapid quenching of the reactions by addition of NaOH.

From these initial experiments, another interesting phenomenon has emerged, related to solvent effects. Indeed, reactions performed with catalyst **3b** in oxygenated solvents such as dioxane, Et_2O or MTBE (entries 7-10), provided the *O*-addition product **6am** with increased ee and opposite configuration, with respect to reactions carried out in CH_2Cl_2, while the absolute configuration of the C-addition product **5am** did not change. Moreover, in oxygenated solvents, neither changes of the product ratios over the time, nor erosion of the enantiomeric excess were observed, despite prolonged reaction times. It should be noted that complementary experiments using indole as the nucleophile instead of 2-naphthol (See Scheme S5 in the ESI) show that reactions in ethers do not give inversion of configuration with respect to reactions in DCM or toluene.[7a]

Scheme 2: Reactions of yne-enones with substituted 1- and 2-naphthols

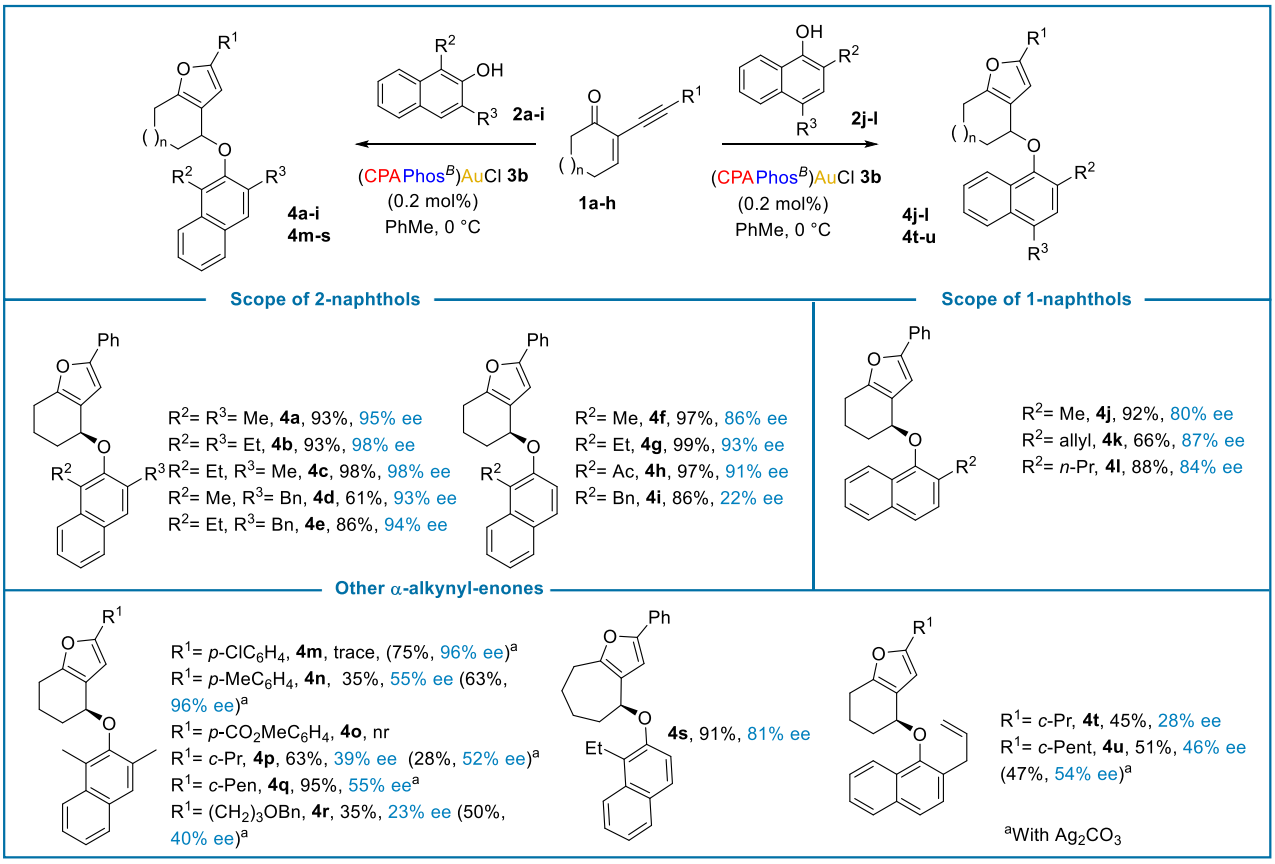

This indicates that the stereochemical control in entries 7-9 (Table 2) should result from a special arrangement of the three-component aggregate formed by the yne-enone-derived carbocationic intermediate (see scheme 1, Eq. 1), the ethereal solvent and 2-naphthol.

The absolute configuration of **6am** was assigned by X-ray diffraction studies (Figure 1). Thus, it could be established that reactions in CH_2Cl_2 or toluene provide (*S*)-configured **6am** while in ethereal solvents the (*R*)-configured **6am** is obtained. Further experiments that will be discussed later in the paper, also established that the *C*-addition product **5am** is (*S*)-configured.

Table 2: Optimization of the reaction between 1a and 2-naphthol

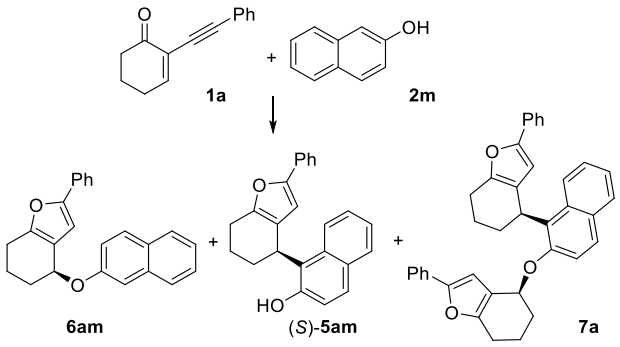

Standard conditions:
1a:**2m** = 1:1; 1 mol% (*S*)-**3a** or (*S*)-**3b**, in CH_2Cl_2 at r.t.

	Cat.	Conditions[#]	Time	Ratio[a]	Ee(%)[b]	
				6am/5am/7a	**6am**	**5am**
1	3a	-	2 min	63/37/0	82 (-)	92 (-)
2	3a	-	30 min	43/57/0	60 (-)	70 (-)
3	3b[c]	-	1 min	49/48/3	33 (-)	91 (-)
4	3b[c]	-	30 min	53/21/26	22 (-)	nd
5	3b[c]	10 °C	5 min	35/65/0	46 (-)	92 (-)
6	3a	in toluene	4 min	63/37/0	85 (-)	94 (-)
7[d]	3b[c]	in dioxane	16 h	70/23/7	77 (+)	90 (-)
8[d]	3b[c]	15 °C, in dioxane	16 h	78/22/0	82 (+)	nd
9[d]	3b[c]	15 °C, in Et_2O	1.5 h	70/30/0	85 (+)	90 (-)
10[d]	3b[c]	15 °C, in MTBE	1.5 h	85/15/0	87 (+)	92 (-)

[#] Variations from standard conditions. [a] Measured by ^1H NMR in the crude mixtures, for quantitative conversion rates. [b] Enantiomeric excesses were measured by chiral HPLC, in most cases from mixtures of **6am** and **5am**. The sign of the optical rotation is given in parentheses for pure, isolated samples, in $CHCl_3$. [c] Reactions performed in the presence of molecular sieves.[13] [d] Reactions performed with a 1.5:1 **1a**/**2m** ratio.

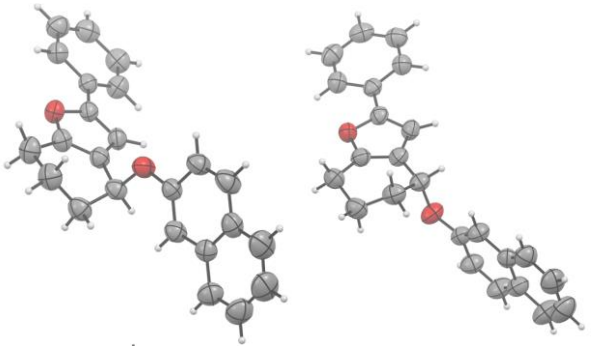

(-)-(*S*)-**6am** (+)-(*R*)-**6am**

Figure 1. X-ray crystal structures of compounds (*S*)-6am from entry 5 and (*R*)-6am from entry 9 in Table 2.

Overall, these experiments have highlighted suitable conditions for the obtention of highly enantioenriched *O*-addition and *C*-addition products **6am** and **5am** respectively:

- (*S*)-(-)-**6am**: catalyst **3a**, in CH_2Cl_2, rt, 1 min (entry 1, conditions A). The product was isolated in 51% yield and 85% ee from a reaction carried out at a 0.5 mmol scale (Scheme 3).
- *(S*)-(-)-**5am**: catalyst **3b**, in CH_2Cl_2, 10°C, 5 min (entry 5, conditions B). The product was isolated in 60% yield and 93% ee at a 0.5 mmol scale (Scheme 3)
- (*R*)-(+)-**6am**: catalyst **3b**, in Et_2O, 15°C, 1.5 h (entry 9, Conditions C). The product could be isolated in >90% yield and 85% ee when the reaction was carried out at a 0.5 mmol scale in the presence of Ag_2CO_3 (Scheme 3)

Scheme 3: Scope of the reactions between cyclic α-ethynyl-enones and 2-naphthols

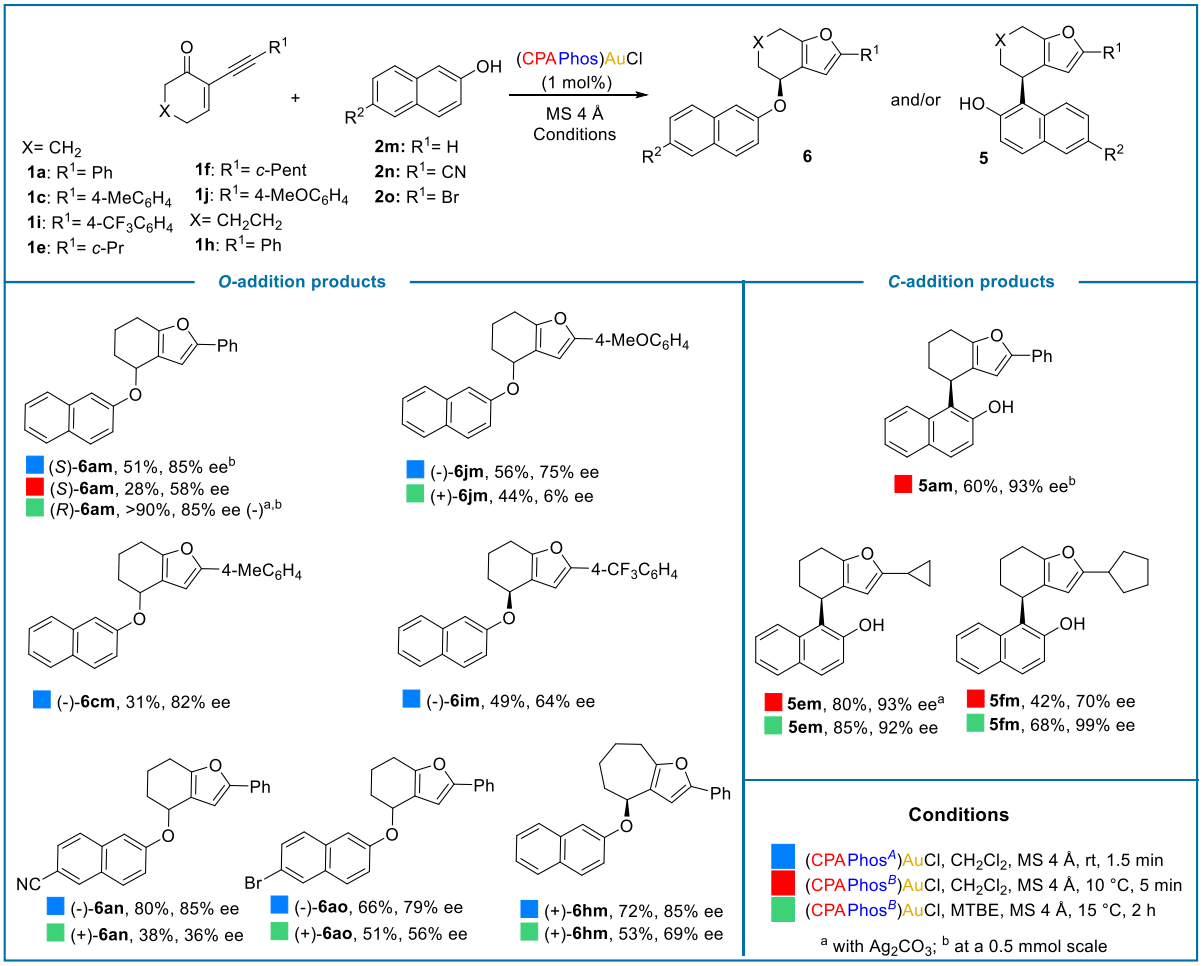

The scope of the method has been explored briefly, as shown in Scheme 3. Conditions A, B or C have been applied to attain the best ee/yield for each product. Either (*S*)-(CPAPhos^{A})AuCl **3a** or (*S*)-(CPAPhos^{B})AuCl **3b** were used as catalysts at a 1 mol% loading, with or without silver carbonate as the additive (see SI for full details). The replacement of the phenyl by an electron-rich *p*-MeOPh group afforded compound **6jm** in 56% yield and 75% ee. The use of an ethereal solvent promoted the formation of the (*R*) enantiomer, but only with 6% ee. When the electron-richness of the aryl group is lower, the enantioselectivity proved higher using the blue conditions (**6cm**, 31% yield, 82% ee).

The reaction proved compatible with electron-withdrawing groups, such as *p*-CF_3Ph, leading to **6im** in 64% ee. 6-Cyanonaphthol and 6-bromonaphthols were used and led to **6an** and **6ao** in good enantioselectivities (85% ee and 79%ee, respectively). Ethereal solvent once again promoted the formation of the opposite enantiomer, even if the level of enantioselectivity is not as high as that in chlorinated solvent.

Starting from the seven-membered-ring enone **1h** we could prepare the *O*-addition product **6b** in 72% yield and 85% ee in CH_2Cl_2, under conditions A. Interestingly, in this case, the use of MTBE did not induce inversion of stereochemistry, as observed for **6a** but furnished the same enantiomer **6b** in 69% ee. Additional *C*-addition products **5** were obtained as the major regioisomers under conditions B. Noteworthy, the reaction with 2-naphthol **2m** tolerates alkyl groups on the alkyne unit of the yne-enones **1**. The *C*-addition products **5em** and **5fm**, featuring cyclopropyl and cyclopentyl groups, were formed as the major products, in good yields and excellent enantioselectivities (92% and 99% ee respectively), under conditions B. Unexpectedly, with these alkyl-substituted yne-enones, conditions C (reactions in Et_2O) also afforded the *C*-addition products as the major products, in excellent yields and even higher enantioselectivities than conditions B.[14]

In further experiments, the cycloisomerization/addition reaction on the yne-enone **1a** has been carried out with 1-naphthol **2p**, as the nucleophile (Scheme 4). The corresponding *O*-addition product **6ap** was obtained in moderate yield, with up to

88% ee, under conditions A, and the *C*-addition product **5ap** was obtained in 61% yield and 98% ee, under conditions B. For both, the absolute configuration was attributed by analogy with that of the corresponding products **5am** and **6am**. The use of an ethereal solvent (with catalyst **3b**) led to the *O*-addition product **6ap** with opposite configuration, in 50% ee. Again, under conditions A, the use of Ag_2CO_3 as an additive provided higher *O*/*C* ratio, while maintaining an excellent level of enantioselectivity (50% yield, 86% ee).

Scheme 4: Optimization of the reaction between 1a and 1-naphthol

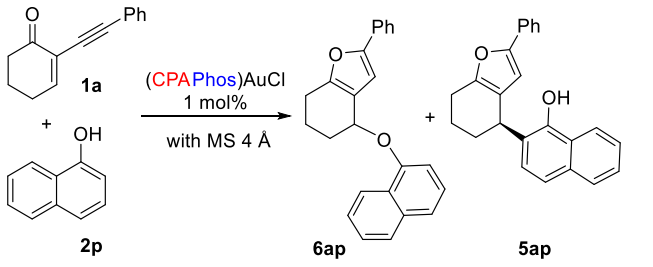

Conditions A:	36%, **88% ee**, (+)-(*S*)	26%, **93% ee**, (*R*)
Conditions A[a]:	50%, **86% ee**, (+)-(*S*)	23%, **97% ee**, (*R*)
Conditions B:	29%, **89% ee**, (+)-(*S*)	61%, **98% ee**, (*R*)
Conditions C:	55%, **50% ee**, (-)-(*R*)	29%, **16% ee**, (*R*)
in Et_2O:	62%, **22% ee**, (-)-(R)	18%, **41% ee**, (*R*)

Reactions carried out on 0.3 mmol **2p**. [a] With Ag_2CO_3

Overall, the reaction of **1a** with 1-naphthol follows the same trend as the reaction with 2-naphthol, in terms of solvent effect: inversion of configuration of the O-addition product in ethereal solvents with respect to DCM.

As noticed in the preliminary experiments (Table 2), two successive cycloisomerization-addition reactions can take place when 2-naphthol **2m** reacts with an excess of enone **1a**, leading to **7a**. In order to establish whether **7a** originates from the *O*-addition product **6am** or from the *C*-addition product **5am**, both compounds were reacted with ketone **1a** (1 equiv) in the presence of a catalytic amount of (CPAPhos^B)AuCl (0.2 mol%). The bis-furane was obtained from **5am** in 72% yield and 85/15 diastereomeric ratio after 15 min at 10 °C, while the *O*-addition product **6am** did not react under these conditions (see Fig S1 in the Supporting Information). Therefore, in order to isolate **7a**, the reaction has been carried out in conditions B, known to favor the *C*-addition product, with a **1a**:**2m** = 2.5:1 ratio. At a 0.5 mmol scale with (CPAPhos^B)AuCl **3b** as the catalyst (1 mol %), in DCM at 10 °C for 15 min, the reaction afforded the bis-furane derivative **7a** in 51% yield and 97% ee, as an inseparable 84:16 mixture of diastereomers (Scheme 5). A 39% amount of the *O*-addition product **6am** was also isolated under these conditions.

Scheme 5: Synthesis of the bis-furane 7a through sequential *C*- and *O*-addition on 2-naphthol.

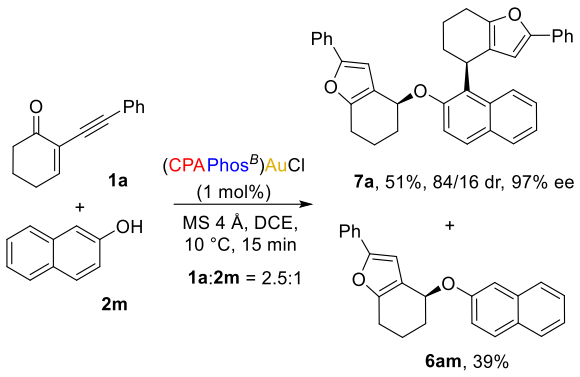

In the last part of our work, we have targeted an asymmetric variant of the α-ethynyl-enone cycloisomerization / 2-naphthol addition / oxidation sequence reported by Ren under silver(I) catalysis (see Scheme 1).[10] In this process, the first formed bicyclic furane **5** (naphthol *C*-addition product) is converted *in situ* into the chiral cyclohexanone **8** by air oxidation (Scheme 6). Therefore, starting from enone **1a** (R^1 = Ph) and 2-naphthol **2m**, we have applied catalytic conditions favoring the *C*-addition pathway. The reaction was carried out in DCM, with (CPAPhos^B)AuCl as the catalyst, and quenched with aqueous sodium hydroxide after only 5 min, since a short reaction time is essential to produce **5** in high ee. The oxidation step has been carried out then in the presence of AgTFA that has been shown to accelerate the oxidation reaction.[10] This two-step protocol led to the desired oxidized product **8am** in 45% yield and 93% ee (Scheme 6). The *O*-addition product **6am** has been isolated also in 22% yield and 52% ee.[15]

Scheme 6: The enantioselective cycloisomerization/addition/oxidation sequence leading to 8

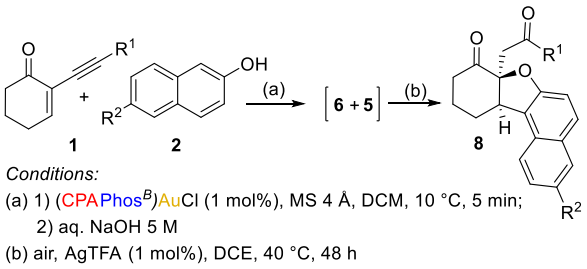

Conditions:
(a) 1) (CPAPhos^{B})AuCl (1 mol%), MS 4 Å, DCM, 10 °C, 5 min;
2) aq. NaOH 5 M
(b) air, AgTFA (1 mol%), DCE, 40 °C, 48 h

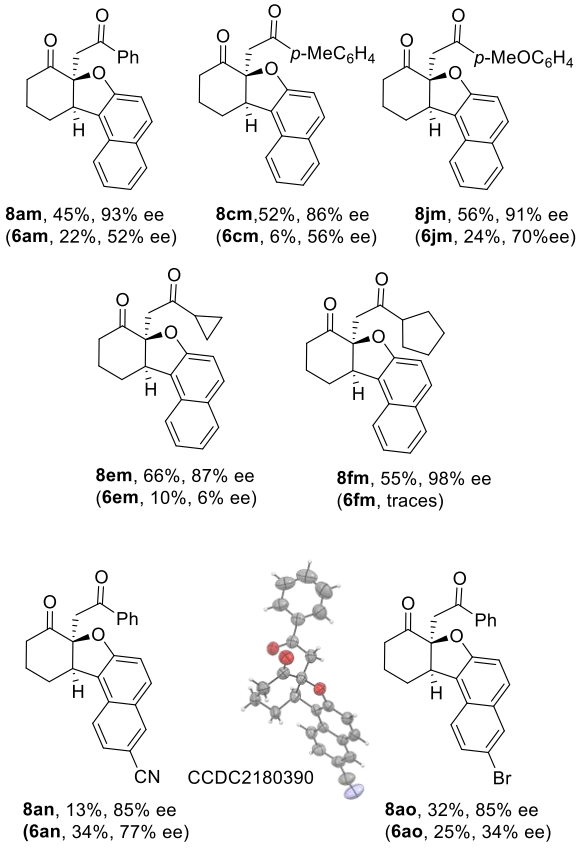

The scope of the reaction has been outlined then briefly. The replacement of the Ph group of **1a** by *p*-tolyl or *p*-methoxyphenyl groups resulted in the formation of **8cm** in 52% yield and 86% ee and **8jm** in 56% yield and 91% ee, respectively. Gratifyingly, enones with aliphatic R^1 substituents (cyclopropyl and cyclopentyl) could be used also, leading to **8em** and **8fm**[16] in good yields and 87% and 98% ee, respectively. 6-Cyanonaphthol **2n** was reacted next with ketone **1a**, delivering compound **8an** in a low 13% yield and 85% ee. However, the isolation of this compound provided a key information, as it enabled the unambiguous assignment of its (*7S,11R*) absolute configuration by X-ray diffraction. By extension, the absolute configuration of the other *C*-addition products **5** could be tentatively assigned. The use of 6-bromonaphthol, less electron-deficient than its cyano analog, led to the final product **8ao** in 32% yield and 85% ee.

Overall, this gold-based protocol expands and improves in terms of enantioselectivity, the silver-based approach previously reported by Ren that led to **8a** in a maximum 42% ee.[10]

As said before, we have found that in the reactions between **1** (R^1 = Ar) and 2-naphthols, prolonged reaction times in DCM favor the *C*-addition product **5am** *vs* O-addition product **6am**, while the enantiomeric excesses of both **5** and **6** decrease over the time. Since these reactions have demonstrated synthetic usefulness, it seemed worth to carry out a few additional experiments to enlighten the above time-dependence of product ratios and ees.

At first, a sample of the *O*-addition product (*S*)-**6am** (80% ee) was treated with 1 mol% of the chiral catalyst (*S*)-(CPAPhos^{B})AuCl **3b** in DCM at r.t. and the mixture was monitored by ^{1}H NMR and chiral HPLC over 1h timespan (Scheme 7, eq. 1 and Figure S2). Compound **6am** evolved over the time into the *C*-addition product **5am**, reaching an approximate 1/1 ratio after 1 h. The enantiomeric excess of (*S*)-**6am** decreased concurrently from 80% to 22%. The *C*-addition product (*S*)-**5am** was formed initially with a 51% ee (after 15 min[17]) but the ee decreased slightly over the time, leading to 34% ee after 1 h.[18] The same trend was observed using (*S*)-(CPAPhos^{A})AuCl **3a**, despite a slower process (see Figure S3). On the contrary, when enantioenriched (*S*)-**6am** was treated with the chiral catalyst (*S*)-**3b**, in the presence of Ag_2CO_3, the starting (*S*)-**6am** remained untouched (see Figure S4a). This experiment suggests that the phosphoric acid function of the (CPAPhos)AuCl catalyst is likely to be responsible for the whole process, which was also confirmed by the use of 1,1'-binaphthyl-2,2'-diyl hydrogenphosphate as the acidic catalyst (see Figure S4b). Interestingly, additional control experiment have shown that concurrent use of CPAPhosAuCl and silver carbonate in the presence of an excess of naphthol (which are the actual reaction conditions) can restore the epimerizing pathway over time (See Figure S4c), presumably by reprotonation of the basic phosphate catalyst. This explains why short reaction times are necessary.

On the other hand, a sample of enantioenriched *C*-addition product (-)-**5a** remained unchanged in the presence of the acidic (CPAPhos)AuCl catalyst (See Figure S5), demonstrating the configurational and structural stability of compounds **5** under these conditions.

Scheme 7: control experiments on the structural and configurational stability of 6am

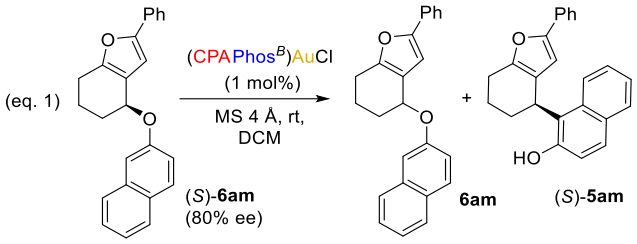

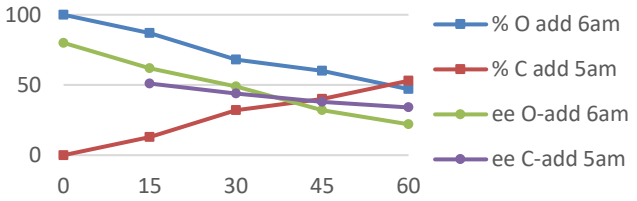

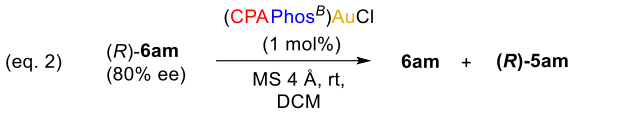

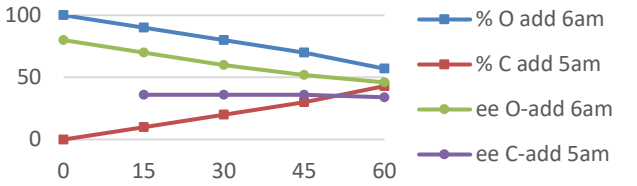

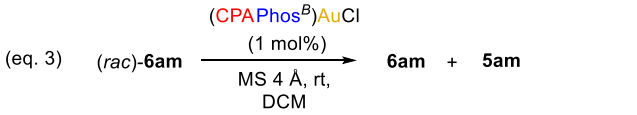

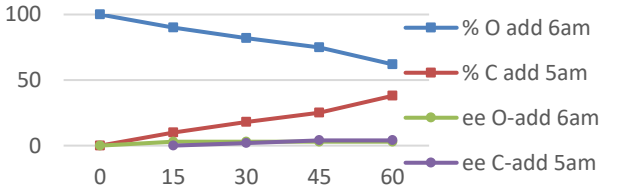

We next exposed the (*R*)-enantiomer of **6am** to complex (*S*)-**3b** and observed a decrease of the ee from 80% to 46%, while (*R*)-**5am** was formed with a 34% ee (Scheme 7, eq. 2 and Figure S6). Under the same conditions, *rac*-**6am** produced nearly racemic **5am**, showing that the stereochemical control does not arise from the chiral Au(I) catalyst (*S*)-**3a**, but mainly from a chirality transfer from the substrate (Scheme 7, eq. 3 and Figure S7).

Another experiment provided crucial information. The compound **6am** was reacted with 1-naphthol **2p** in the presence of complex (*S*)-**3b** and the composition of the mixture was monitored by ^{1}H NMR over 2.5 h (Scheme 8 and Figure S8). It was found that after 30 min, the mixture contained only 23% of the starting material and 38% of the neoformed *C*-addition product **5am**, together with the two 1-naphthol derived compounds **6ap** (23%) and **5ap** (16%). Both *O*-addition products **6am** and **6ap** had virtually disappeared after 2.5 h, in favor of the formation of the corresponding *C*-addition products **5am** and **5ap**. These results attest for a reaction pathway involving cleavage of the C-O bond of the starting material **6am** via an intermolecular process.

Scheme 8: Evidence for an intermolecular exchange process by cross experiments

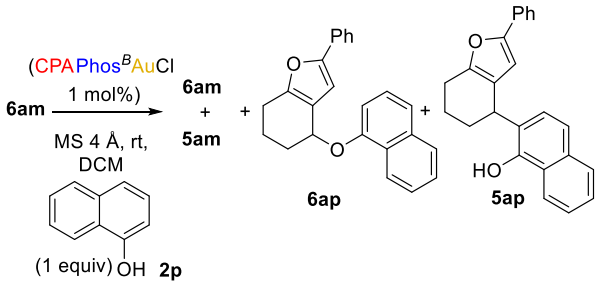

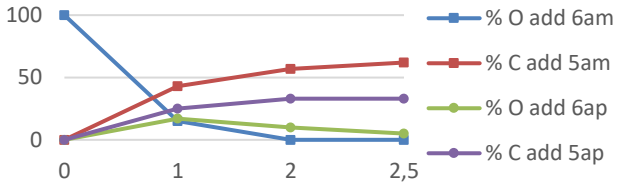

Overall, these experiments show that enantioenriched **5am** can be formed from enantioenriched **6am** *via* a stereoretentive mechanism promoted by the acid catalyst (chirality transfer). However, over the time, the acidic function of the catalyst also triggers the erosion of the ee of **6am** and, consequently, the erosion of the ee of **5am**.

On the basis of these experiments, we pictured a plausible mechanism accounting for the outcomes of the catalytic reactions, including the erosion of the enantiomeric excess of compound **6am** and its conversion into **5am** (Scheme 9). We know that both products **5am** and **6am** are formed initially with high enantioselectivity from the Au-promoted reaction (high ees for short reaction times). The final products (*S*)-**6am** and (*S*)-**5am**) might results from the preferred conformation of intermediate ***i*** that is formed in the cycloisomerization step. As shown in our previous reports,[7a, 7c] the lowest energy form of the intermediate carbocation ***i*** presents a free pro-(*S*) face where the naphthol nucleophile will add preferentially.

However, compound **6am** can be H-bonded by the acidic catalyst (CPAPhos)AuCl **3**, which results in the formation of intermediate ***ii***. Intermediate ***ii*** evolves then into intermediate ***iii*** by cleavage of the C-O bond and proton transfer, thereby losing

the stereogenic center. Our experiments indicate that two different pathways are then operating concurrently: (1) the reversible cleavage of the C-O bond that generates the racemic *O*-addition product **6am** (supported by eq. 1 and 2 of Scheme 7) and (2) the intramolecular formation of the *C*-addition product, that proceeds with chirality transfer and leads to enantioenriched, (*S*)-configured **5am** (as supported by eq. 1 and 2 in Scheme 7). The chiral gold catalyst does not provide any significant chiral induction at this step, as shown by the experiment on racemic **6am** (eq. 3, Scheme 7). [19]

The final ees and ratio of **5am** and **6am** hence might depend on the magnitude and/or control of these concurrent processes, as a function of the substrates and reaction conditions.

To gain better insight into the erosion of the enantioselectivity and the structural instability of the *O*-addition products **6**, we have carried out a computational study at the DFT level (see SI for computational details). The calculations started from product (*S*)-**6am** and the BINOL-derived chiral phosphoric acid (*S*)-**3c** (Figure 2), as a model of the phosphoric acid unit of (*S*)-**3a**, for which we have shown that it catalyzes the same rearrangement (see Figure S4b). **6am** binds to **3c** through *H*-bonding, forming **9a**. This complex can evolve, via the breaking of a C-O bond and a proton transfer, to form pro-(*S*)-**10a**. This carbocationic intermediate retains the initial stereochemical information, due to the interaction between the naphthol oxygen and the cationic site. This interaction induces a 51.1 kJ/mol stabilization of **10a** with respect to the dissociated ion pair **11a** · **12**.

Although dissociation of **10a** into **11a** · **12** is highly endothermic (112.7 kJ/mol from **9a**, 51.1 kJ/mol from the analogous intermediate **10a**), it is likely to be responsible for the racemization of (*S*)-**6am**, since the stereochemical information is lost in the carbocation and the subsequent *O*-addition of naphthol can take place from both faces (the whole energetic pathways to reach pro-(*R*)-**6am** is given in the ESI, Scheme S7). At room temperature, this barrier is difficult to cross while remaining accessible, which explains why this process is slow (see Scheme 7). It should be noted that for R^1 = *c*-Pr, this process is significantly less endothermic (101.2 kJ/mol, see ESI, Scheme S8), leading to a much faster loss of the chiral information, which fits with the low ee obtained for this type of substrate (see Scheme 2).

Alternatively, intermediate **10a** can also change its geometry. In particular, the naphthol and the cyclic cationic moieties, both approximately planar and located in parallel planes, can shift relative to each other, leading to pro-(*S*)-**13a** where the cationic site interacts preferentially with the electron-rich carbon of the naphthol. **13a** retains the chiral information present in **6am**, **9a** and **10a**. The formation of the C-C bond followed by re-aromatization of the naphthol moiety leads to (*S*)-**5am** in 2 steps from **13**a.

Overall, the conversion of **6am** to **5am** is exothermic by 22.9 kJ/mol, which explains the irreversible formation of the *C*-addition product. However, the activation barrier of this process is high (107.6 kJ/mol from **9a**), which explains why the conversion of *O*- to *C*-product is slow.[20]

Finally, it is of note that the same epimerizing process occurs in the reactions using substituted naphthols (See Scheme S6 in the ESI), probably via a similar mechanism, that we have not computed. The increased steric hindrance of naphthols **2a-l** results in slower kinetics, which increases the competing epimerizing process, explaining the moderate enantioselectivities obtained with certain naphthols (see Scheme 2).

In summary, we have shown that the tandem cycloisomerization/naphthol addition reactions on □-ethynyl-cyclic enones **1** are promoted by the CPAPhosAuCl complexes at low 0.2-1 mol % catalyst loading. Substituted 1- and 2-naphthols behave as *O*-nucleophiles and produce highly enantioenriched bicyclic furans (14 examples, ee>80%). The parent naphthols produce both *O*- and *C*-addition products in high ees. In the presence of acids, the *O*-addition products convert into the *C*-addition products with concomitant decrease of the enantiomeric excess. Finally, the *C*-addition products **5** could be oxidized *in situ* into the corresponding bicyclic ketones **8** without eroding their enantiomeric excess.

Despite the fact that these reactions required considerable optimization and deep understanding of mechanistic pathways, silver-free conditions are worth seeking. It is indeed well-established that the gold counterion originating from the silver salt has dramatic impact on reaction outcomes.[21] More importantly, it has been demonstrated many times that the role of the residual silver salts is rarely innocent in Au(I) catalysis.[1a, 22] There is hence an undeniable interest to the development of silver-free strategies in Au(I) catalysis,[23] some of them proceeding by the design of complexes that can self-activate by a hydrogen bond assistance, [24] as it is the case in our CPAPhosAuCl series.[7a, 7c] The silver-free reactions developed hereby guarantee a true gold-catalyzed catalytic cycles in addition to save the costs of expensive silver salts.

Thus, in the end, our gold catalysts featuring a hybrid phosphine-phosphoric acid ligand (CPAPhos) enable the access to a wide range of highly enantioenriched bicyclic furanes and, indirectly, to the corresponding functionalized ketones via air oxidation.

Acknowledgements

This work has been supported in part by the ANR funding agency *via* the collaborative project "BiAuCat" (ANR-20-CE07-0037). We thank the China Scholarship Council for PhD funding to Y. Y. and Z. Z., the ANR for the Post-doctoral fellowship to N.S. and PhD fellowship of M. D. and the GDR Phosphore for support.

Scheme 9: Proposed pathways for the epimerization of 6 and the conversion of 6am into 5am.

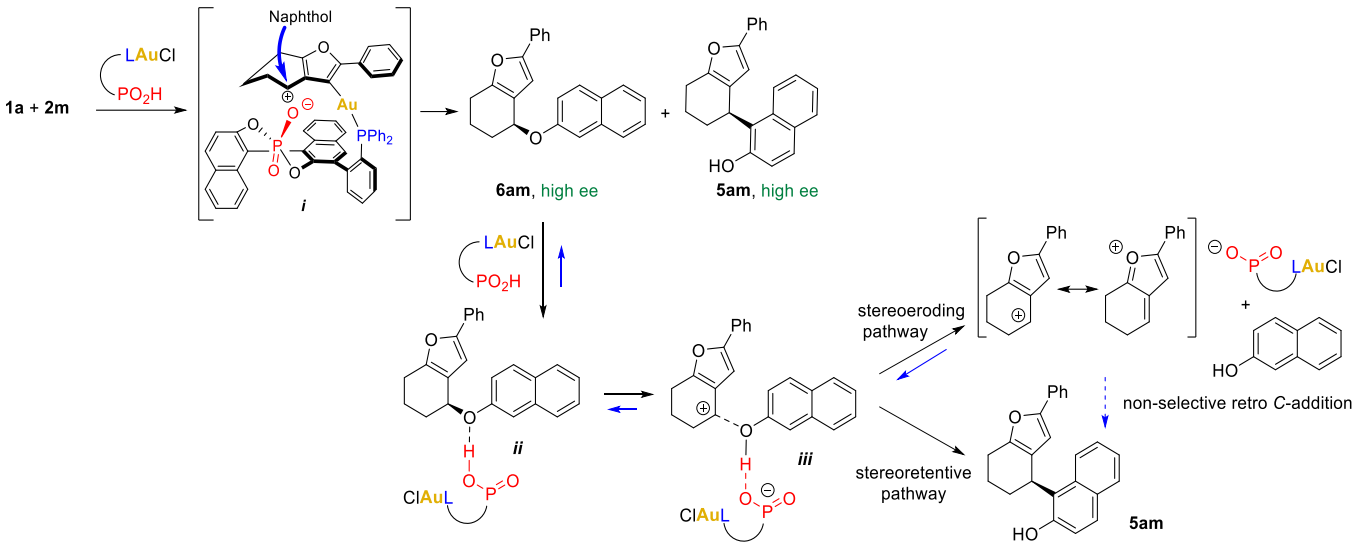

Figure 2. Schematic potential energy surface (Gibbs free energy in kJ mol^{-1}) for the erosion of the enantioselectivity and the structural instability of the *O*-addition product 6am obtained at the IEFPCM(DCM)-M06/Def2-TZVPP//IEFPCM(DCM)-M06/Def2-SVP level.

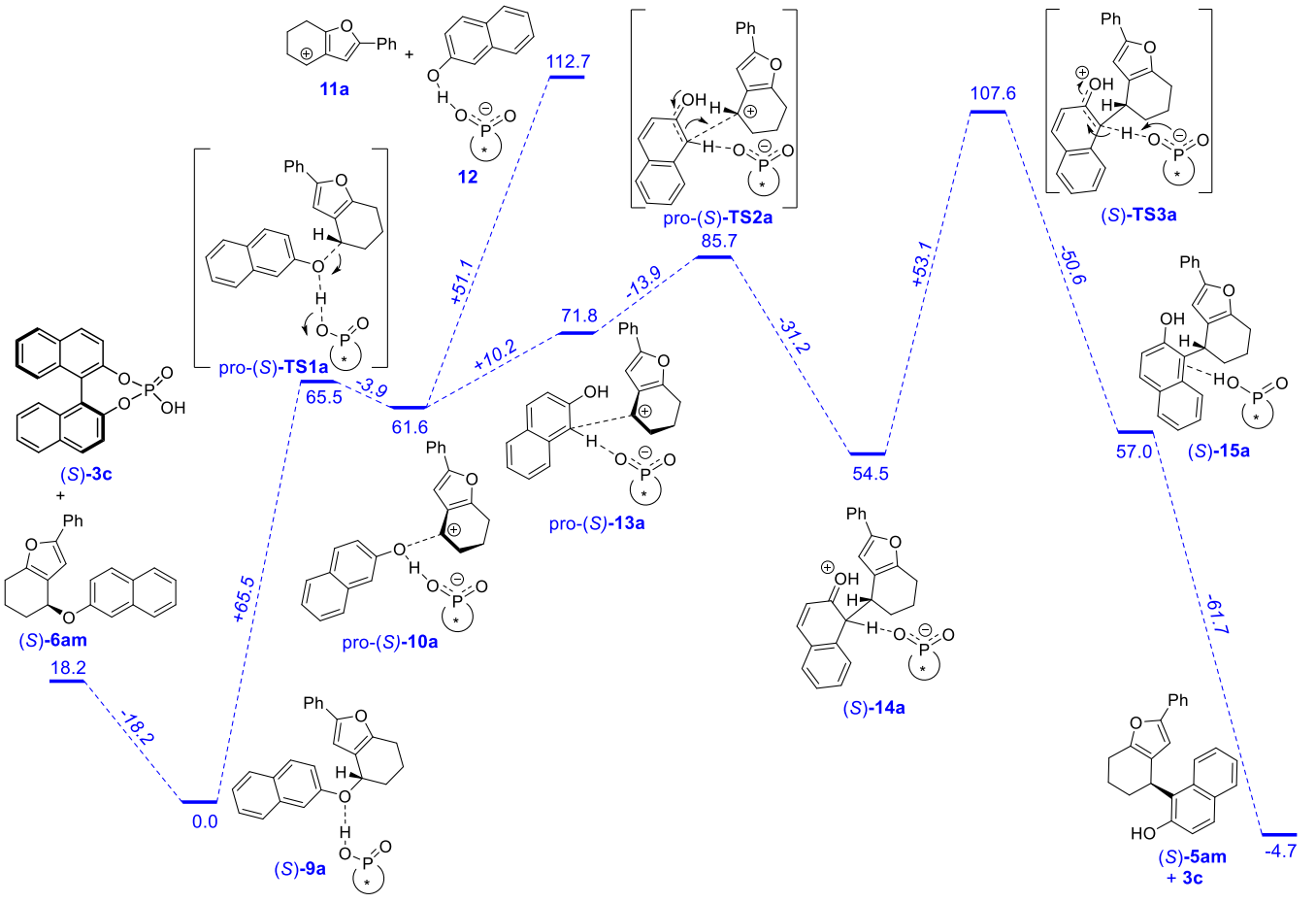

References

1. (a) Ranieri, B.; Escofet, I.; Echavarren, A. M., Anatomy of gold catalysts: facts and myths. *Org. Biomol. Chem.* **2015,** *13*, 7103; (b) Hashmi, A. S. K.; Hutchings, G. J., Gold catalysis. *Angew. Chem. Int. Ed.* **2006,** *45*, 7896; (c) Hashmi, A. S. K., Gold-Catalyzed Organic Reactions. *Chem. Rev.* **2007,** *107*, 3180; (d) Gorin, D. J.; Sherry, B. D.; Toste, F. D., Ligand effects in homogeneous Au catalysis. *Chem. Rev.* **2008,** *108*, 3351; (e) Wang, W.; Hammond, G. B.; Xu, B., Ligand Effects and Ligand Design in Homogeneous Gold(I) Catalysis. *J. Am. Chem. Soc.* **2012,** *134*, 5697; (f) Ding, D.; Mou, T.; Feng, M.; Jiang, X., Utility of Ligand Effect in Homogenous Gold Catalysis: Enabling Regiodivergent π-Bond-Activated Cyclization. *J. Am. Chem. Soc.* **2016,** *138*, 5218.

2. (a) Sengupta, S.; Shi, X., Recent Advances in Asymmetric Gold Catalysis. *ChemCatChem* **2010,** *2*, 609; (b) Pradal, A.; Toullec, P. Y.; Michelet, V., Recent Developments in Asymmetric Catalysis in the Presence of Chiral Gold Complexes. *Synthesis* **2011**, 1501; (c) Cera, G.; Bandini, M., Enantioselective Gold(I) Catalysis with Chiral Monodentate Ligands. *Isr. J. Chem.* **2013,** *53*, 848; (d) Wang, Y.-M.; Lackner, A. D.; Toste, F. D., Development of Catalysts and Ligands for Enantioselective Gold Catalysis. *Acc. Chem. Res.* **2014,** *47*, 889; (e) Zi, W.; Toste, D. F., Recent advances in enantioselective gold catalysis. *Chem. Soc. Rev.* **2016,** *45*, 4567; (f) Li, Y.; Li, W.; Zhang, J., Gold-Catalyzed Enantioselective Annulations. *Chem. Eur. J.* **2017,** *23*, 467.

3. (a) Magné, V.; Sanogo, Y.; Demmer, C. S.; Retailleau, P.; Marinetti, A.; Guinchard, X.; Voituriez, A., Chiral Phosphathiahelicenes: Improved Synthetic Approach and Uses in Enantioselective Gold(I)-Catalyzed [2+2] Cycloadditions of *N*-Homoallenyl Tryptamines. *ACS Catal.* **2020,** *10*, 8141; (b) Glinsky-Olivier, N.; Yang, S.; Retailleau, P.; Gandon, V.; Guinchard, X., Enantioselective Gold-Catalyzed Pictet–Spengler Reaction. *Org. Lett.* **2019,** *21*, 9446; (c) Magné, V.; Lorton, C.; Marinetti, A.; Guinchard, X.; Voituriez, A., Short Enantioselective Total Synthesis of (-)-Rhazinilam Using a Gold(I)-Catalyzed Cyclization. *Org. Lett.* **2017,** *19*, 4794; (d) Wu, Z.; Isaac, K.; Retailleau, P.; Betzer, J.-F.; Voituriez, A.; Marinetti, A., Planar Chiral Phosphoramidites with a Paracyclophane Scaffold: Synthesis, Gold(I) Complexes, and Enantioselective Cycloisomerization of Dienynes. *Chem. Eur. J.* **2016,** *22*, 3278; (e) Aillard, P.; Retailleau, P.; Voituriez, A.; Marinetti, A., Synthesis of New Phosphahelicene Scaffolds and Development of Gold(I)-Catalyzed Enantioselective Allenene Cyclizations. *Chem. Eur. J.* **2015,** *21*, 11989; (f) Magné, V.; Marinetti, A.; Gandon, V.; Voituriez, A.; Guinchard, X., Synthesis of Spiroindolenines via Regioselective Gold(I)-Catalyzed Cyclizations of *N*-Propargyl Tryptamines. *Adv. Synth. Catal.* **2017,** *359*, 4036.

4. Hamilton, G. L.; Kang, E. J.; Mba, M.; Toste, F. D., A Powerful Chiral Counterion Strategy for Asymmetric Transition Metal Catalysis. *Science* **2007,** *317*, 496.

5. (a) Taylor, M. S.; Jacobsen, E. N., Asymmetric catalysis by chiral hydrogen-bond donors. *Angew. Chem. Int. Ed.* **2006,** *45*, 1520; (b) Mayer, S.; List, B., Asymmetric Counteranion-Directed Catalysis. *Angew. Chem. Int. Ed.* **2006,** *45*, 4193; (c) Mahlau, M.; List, B., Asymmetric Counteranion-Directed Catalysis: Concept, Definition, and Applications. *Angew. Chem. Int. Ed.* **2013,** *52*, 518.

6. (a) Aikawa, K.; Kojima, M.; Mikami, K., Synergistic Effect: Hydroalkoxylation of Allenes through Combination of Enantiopure BIPHEP-Gold Complexes and Chiral Anions. *Adv. Synth. Catal.* **2010,** *352*, 3131; (b) Barreiro, E. M.; Broggini, D. F. D.; Adrio, L. A.; White, A. J. P.; Schwenk, R.; Togni, A.; Hii, K. K., Gold(I) Complexes of Conformationally Constricted Chiral Ferrocenyl Phosphines. *Organometallics* **2012,** *31*, 3745; (c) Miles, D. H.; Veguillas, M.; Toste, F. D., Gold(I)-catalyzed enantioselective bromocyclization reactions of allenes. *Chem. Sci.* **2013,** *4*, 3427; (d) Spittler, M.; Lutsenko, K.; Czekelius, C., Total Synthesis of (+)-Mesembrine Applying Asymmetric Gold Catalysis. *J. Org. Chem.* **2016,** *81*, 6100; (e) Handa, S.; Lippincott, D. J.; Aue, D. H.; Lipshutz, B. H., Asymmetric Gold-Catalyzed Lactonizations in Water at Room Temperature. *Angew. Chem. Int. Ed.* **2014,** *53*, 10658; (f) Aikawa, K.; Kojima, M.; Mikami, K., Axial Chirality Control of Gold(biphep) Complexes by Chiral Anions: Application to Asymmetric Catalysis. *Angew. Chem. Int. Ed.* **2009,** *48*, 6073; (g) LaLonde, R.; Wang, Z.; Mba, M.; Lackner, A.; Toste, F., Gold(I)-Catalyzed Enantioselective Synthesis of Pyrazolidines, Isoxazolidines, and Tetrahydrooxazines. *Angew. Chem. Int. Ed.* **2010,** *49*, 598; (h) Mourad, A. K.; Leutzow, J.; Czekelius, C., Anion-Induced Enantioselective Cyclization of Diynamides to Pyrrolidines Catalyzed by Cationic Gold Complexes. *Angew. Chem. Int. Ed.* **2012,** *51*, 11149; (i) Zi, W.; Toste, F. D., Gold(I)-Catalyzed Enantioselective Desymmetrization of 1,3-Diols through Intramolecular Hydroalkoxylation of Allenes. *Angew. Chem. Int. Ed.* **2015,** *54*, 14447.

7. (a) Zhang, Z.; Smal, V.; Retailleau, P.; Voituriez, A.; Frison, G.; Marinetti, A.; Guinchard, X., Tethered Counterion-Directed Catalysis: Merging the Chiral Ion-Pairing and Bifunctional Ligand Strategies in Enantioselective Gold(I) Catalysis. *J. Am. Chem. Soc.* **2020,** *142*, 3797; (b) Yu, Y.;

Zhang, Z.; Voituriez, A.; Rabasso, N.; Frison, G.; Marinetti, A.; Guinchard, X., Enantioselective Au(I)-catalyzed dearomatization of 1-naphthols with allenamides through Tethered Counterion-Directed Catalysis. *Chem. Commun.* **2021,** *57*, 10779; (c) Zhang, Z.; Sabat, N.; Frison, G.; Marinetti, A.; Guinchard, X., Enantioselective Au(I)-Catalyzed Multicomponent Annulations via Tethered Counterion-Directed Catalysis. *ACS Catal.* **2022,** *12*, 4046.

8. (a) Qian, D.; Zhang, J., Yne–Enones Enable Diversity-Oriented Catalytic Cascade Reactions: A Rapid Assembly of Complexity. *Acc. Chem. Res.* **2020,** *53*, 2358; (b) Bao, X.; Ren, J.; Yang, Y.; Ye, X.; Wang, B.; Wang, H., 2-Activated 1,3-enynes in enantioselective synthesis. *Org. Biomol. Chem.* **2020,** *18*, 7977; (c) Huple, D. B.; Ghorpade, S.; Liu, R.-S., Recent Advances in Gold-Catalyzed N- and O-Functionalizations of Alkynes with Nitrones, Nitroso, Nitro and Nitroxy Species. *Adv. Synth. Catal.* **2016,** *358*, 1348; (d) Siva Kumari, A. L.; Siva Reddy, A.; Swamy, K. C. K., Exploring the gold mine: [Au]-catalysed transformations of enynals, enynones and enynols. *Org. Biomol. Chem.* **2016,** *14*, 6651; (e) Qian, D.; Zhang, J., Gold-Catalyzed Cascade Reactions for Synthesis of Carbo- and Heterocycles: Selectivity and Diversity. *Chem. Rec.* **2014,** *14*, 280.

9. (a) Rauniyar, V.; Wang, Z. J.; Burks, H. E.; Toste, F. D., Enantioselective Synthesis of Highly Substituted Furans by a Copper(II)-Catalyzed Cycloisomerization-Indole Addition Reaction. *J. Am. Chem. Soc.* **2011,** *133*, 8486; (b) Force, G.; Ki, Y. L. T.; Isaac, K.; Retailleau, P.; Marinetti, A.; Betzer, J. F., Paracyclophane-based Silver Phosphates as Catalysts for Enantioselective Cycloisomerization/Addition Reactions: Synthesis of Bicyclic Furans. *Adv. Synth. Catal.* **2018,** *360*, 3356.

10. Li, Z.; Peng, J.; He, C.; Xu, J.; Ren, H., Silver(I)-Mediated Cascade Reaction of 2-(1-Alkynyl)-2-alken-1-ones with 2-Naphthols. *Org. Lett.* **2020,** *22*, 5768.

11. Pielhop, T.; Larrazábal, G.; Rudolf von Rohr, P., Autohydrolysis pretreatment of softwood – Enhancement by phenolic additives and the effects of other compounds. *Green Chem.* **2016,** *18*.

12. (a) Xia, Z.-L.; Xu-Xu, Q.-F.; Zheng, C.; You, S.-L., Chiral phosphoric acid-catalyzed asymmetric dearomatization reactions. *Chem. Soc. Rev.* **2020,** *49*, 286; (b) An, J.; Bandini, M., Recent Advances in the Catalytic Dearomatization of Naphthols. *Eur. J. Org. Chem.* **2020,** *2020*, 4087.

13. Water acts as a nucleophile in this reaction and should be avoided. See ref. 7a.

14. It should be noted that *C*-addition products **5jm**, **5an** and **5ao** can be obtained using conditions B, but are prone to oxidation. This has been further exploited in this work, see Scheme 6.

15. All products **6** formed as by-products in these reactions are indicated in brackets.

16. The first step was performed in MTBE, since these conditions give the highest ee for the intermediate compound **5fm**.

17. The ee of **5am** could not be measured at earlier reaction time because of the low conversion of **6am** in **5am**.

18. The same reaction performed using Au(I) complex **3a** lead to similar results. See Figure S3 in the ESI).

19. Additional experiment was performed from *rac*-**6am** using TRIP as a chiral phosphoric acid, which equally resulted in the formation of virtually racemic compounds.

20. Furthermore, we assume that a similar reaction pathway occurs from pro-(*R*)-**10a** to account for the experimentally observed formation of (*R*)-**5am**, although this has not been calculated.

21. (a) Lu, Z.; Li, T.; Mudshinge, S. R.; Xu, B.; Hammond, G. B., Optimization of Catalysts and Conditions in Gold(I) Catalysis—Counterion and Additive Effects. *Chem. Rev.* **2021,** *121*, 8452; (b) Lu, Z.; Hammond, G. B.; Xu, B., Improving Homogeneous Cationic Gold Catalysis through a Mechanism-Based Approach. *Acc. Chem. Res.* **2019,** *52*, 1275; (c) Schiessl, J.; Schulmeister, J.; Doppiu, A.; Woerner, E.; Rudolph, M.; Karch, R.; Hashmi, A. S. K., An Industrial Perspective on Counter Anions in Gold Catalysis: Underestimated with Respect to "Ligand Effects". *Adv. Synth. Catal.* **2018,** *360*, 2493; (d) Schießl, J.; Schulmeister, J.; Doppiu, A.; Wörner, E.; Rudolph, M.; Karch, R.; Hashmi, A. S. K., An Industrial Perspective on Counter Anions in Gold Catalysis: On Alternative Counter Anions. *Adv. Synth. Catal.* **2018,** *360*, 3949; (e) Lu, Z.; Han, J.; Okoromoba, O. E.; Shimizu, N.; Amii, H.; Tormena, C. F.; Hammond, G. B.; Xu, B., Predicting Counterion Effects Using a Gold Affinity Index and a Hydrogen Bonding Basicity Index. *Org. Lett.* **2017,** *19*, 5848; (f) Jaroschik, F.; Simonneau, A.; Lemiere, G.; Cariou, K.; Agenet, N.; Amouri, H.; Aubert, C.; Goddard, J.-P.; Lesage, D.; Malacria, M.; Gimbert, Y.; Gandon, V.; Fensterbank, L., Assessing ligand and counterion effects in the noble metal catalyzed cycloisomerization reactions of 1,6-allenynes: a combined experimental and theoretical approach. *ACS Catal.* **2016,** *6*, 5146; (g) Jia, M.; Bandini, M., Counterion Effects in Homogeneous Gold Catalysis. *ACS Catal.* **2015,** *5*, 1638.

22. (a) Zhdanko, A.; Maier, M. E., Explanation of "Silver Effects" in Gold(I)-Catalyzed Hydroalkoxylation of Alkynes. *ACS Catal.* **2015,** *5*, 5994; (b) Homs, A.; Escofet, I.; Echavarren, A. M., On the Silver Effect and the Formation of

Chloride-Bridged Digold Complexes. *Org. Lett.* **2013,** *15*, 5782; (c) Wang, D.; Cai, R.; Sharma, S.; Jirak, J.; Thummanapelli, S. K.; Akhmedov, N. G.; Zhang, H.; Liu, X.; Petersen, J. L.; Shi, X., "Silver Effect" in Gold(I) Catalysis: An Overlooked Important Factor. *J. Am. Chem. Soc.* **2012,** *134*, 9012; (d) Weber, D.; Gagné, M. R., Dinuclear Gold−Silver Resting States May Explain Silver Effects in Gold(I)-Catalysis. *Org. Lett.* **2009,** *11*, 4962.

23. (a) Franchino, A.; Montesinos-Magraner, M.; Echavarren, A. M., Silver-Free Catalysis with Gold(I) Chloride Complexes. *Bull. Chem. Soc. Jpn.* **2021,** *94*, 1099; (b) Gaillard, S.; Bosson, J.; Ramón, R. S.; Nun, P.; Slawin, A. M. Z.; Nolan, S. P., Development of Versatile and Silver-Free Protocols for Gold(I) Catalysis. *Chem. Eur. J.* **2010,** *16*, 13729.

24. (a) Echavarren, A. M.; Franchino, A.; Martí, À.; Nejrotti, S., Silver-Free Au(I) Catalysis Enabled by Bifunctional Urea- and Squaramide-Phosphine Ligands via H-Bonding. *Chem. Eur. J.* **2021,** *27*, 11989; (b) Schmidbaur, H.; Schier, A., Silver-free Gold(I) Catalysts for Organic Transformations. *Z. Naturforsch. B* **2011,** *66*, 329.